COMMUNICATION

Uranium(IV) Thio- and Selenoether Complexes: Syntheses, Structures, and Computational Investigation of U–ER_2 Interactions

Novan A. G. Gray,[a] Jeffrey S. Price[a] and David J. H. Emslie*[a]

[a] N. A. G. Gray, Dr. J. S. Price, Prof. Dr. D. J. H. Emslie
Department of Chemistry and Chemical Biology
McMaster University
1280 Main Street West, Hamilton, Ontario, L8S 4M1, Canada
E-mail: emslied@mcmaster.ca

Supporting information for this article is given via a link at the end of the document.

Abstract: Rigid thioether- and selenoether-containing pincer pro-ligands, H[AS_2^{Ph2}] (**1**) and H[ASe_2^{Ph2}] (**2**), were synthesized, and deprotonation provided the potassium salts [K(AS_2^{Ph2})(dme)] (**3**) and [K(ASe_2^{Ph2})(dme)$_2$] (**4**). Reaction of two equivalents of **3** or **4** with [UI_4(dioxane)$_2$] afforded the uranium thioether complex [(AS_2^{Ph2})$_2$$UI_2$] (**5**) and the first example of a uranium selenoether complex, [(ASe_2^{Ph2})$_2$$UI_2$] (**6**). X-ray structures revealed distorted square antiprismatic geometries in which the AE_2^{Ph2} ligands are κ^3-coordinated. The nature of U–ER_2 bonding in **5** and **6**, as well as methyl-free analogues of **5** and **6** and a hypothetical ether analogue, was investigated computationally (including NBO, AIM and ELF calculations) illustrating increasing covalency from O to S to Se.

Understanding of actinide–ligand bonding is of importance from a fundamental perspective, and as a means to further the rational development of ligands for lanthanide–actinide separation in nuclear fuel reprocessing.[1,2] Compared with ligands featuring oxygen-donors (e.g. ethers, alkoxides and phosphinates), those containing softer sulfur donors[3] have been shown to be particularly effective for lanthanide–actinide differentiation.[2] This is thought to result from increased covalency in the actinide–soft donor linkages,[4,5,6] enabled by the greater radial extension of the 5*f* versus 4*f* orbitals combined with the increased polarizability and lesser electronegativity of the donor atom.[7] By extension, interactions with heavier chalcogens such as selenium might be expected to be more covalent still. However, very few actinide complexes featuring multidentate ligands incorporating selenium donors have been reported (*vide infra*).

In 2005-2008, Neu, Gaunt, and Kaltsoyannis et al. reported trivalent uranium complexes of monoanionic $N(PR_2S)_2$ and $N(PR_2Se)_2$ ligands (a in Figure 1),[6,8] and DFT calculations indicated increased covalency in the latter, associated primarily with an increase in uranium *d*-orbital character in the U–Se bonds. These imidodiphosphinochalcogenide anions can be represented by several resonance forms, including those which place the negative charge on a chalcogen donor.

Compared with selenium donors bearing a formal negative charge, neutral selenoether donors may be expected to afford *f*-element complexes with a lower total ionic contribution to U–Se bonding. However, uranium–selenoether complexes have not been definitively identified. For example, Lukens and Walensky et al. recently installed dianionic selenoether-containing bis(phenolate) ligands on uranium to form [{(4,6-$^tBu_2C_6H_2O)_2Se\}_2U^{IV}(THF)_2$] (b in Figure 1). However, the oxygen donors afforded an approximately octahedral coordination geometry at uranium, and on the basis of the U–Se distances, the authors concluded that no interactions exist between the selenium atoms and the uranium centre.[9,10]

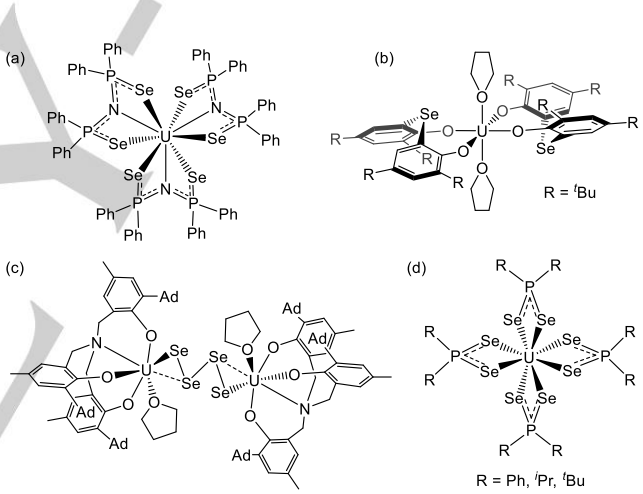

Figure 1. Uranium(III) and (IV) complexes bearing selenium-containing $[N(PPh_2Se)_2]^-$, $[(4,6\text{-}^tBu_2C_6H_2O)_2Se]^{2-}$, $[Se_4]^{2-}$ and $[Se_2PR_2]^-$ ligands.

Nevertheless, uranium–selenium interactions which can be considered to be dative in character have been observed in μ-Se_4^{2-} and $Se_2PR_2^-$ complexes. For example, Boncella et al. reported [{(^{t}BuN)$_2$$U^{VI}$I(^{t}Bu$_2$bpy)}$_2$($\mu$-$\eta^2$:$\eta^2$-$Se_4$)] (^{t}Bu$_2$bpy = 4,4'-di-*tert*-butyl-2,2'-bipyridine),[11] and Franke and Meyer et al. reported [{({^{Ad}ArO}$_3$N)U^{IV}}$_2$(μ-η^3:η^3-Se_4)] and [{({^{Ad}ArO}$_3$N)U^{IV}(THF)}$_2$(μ-η^2:η^2-Se_4)] (c in Figure 1).[12] In all cases, bonds between uranium and the terminal selenium atoms are short, whereas longer dative interactions were proposed between uranium and the central selenium atoms in the Se_4 chain. Additionally, homoleptic [U^{IV}(Se_2PR_2)$_4$] (R = Ph, ^{i}Pr or ^{t}Bu; d in Figure 1) complexes have been synthesized and crystallographically characterized, with one shorter and one longer U–Se distance to each diselenophosphinate ligand.[13,14]

In this work, we report the syntheses of rigid SNS- and SeNSe-donor ligands featuring a central amido anion flanked by neutral chalcogenoether groups. These ligands were used to

access a uranium thioether complex, and the first example of a uranium selenoether complex. Computational investigations into the nature of U–ER_2 bonding are also described, including comparisons with a hypothetical ether analogue.

Palladium-catalyzed cross coupling of 4,5-dibromo-2,7,9,9-tetramethylacridan and one equivalent of diphenyl disulfide in the presence of zinc powder[15] afforded the thioether-containing pro-ligand, H[AS_2^{Ph2}] (**1**). By contrast, the selenoether analogue, H[ASe_2^{Ph2}] (**2**), was synthesized by tri-lithiation of H[ABr_2], followed by addition of diphenyl diselenide and quenching with aqueous HCl (Scheme 1). Pro-ligands **1** and **2** were deprotonated using one equivalent of KCH_2Ph, affording yellow [K(AS_2^{Ph2})(dme)] (**3**) and [K(ASe_2^{Ph2})(dme)$_2$] (**4**) in 57% yield (Scheme 2).

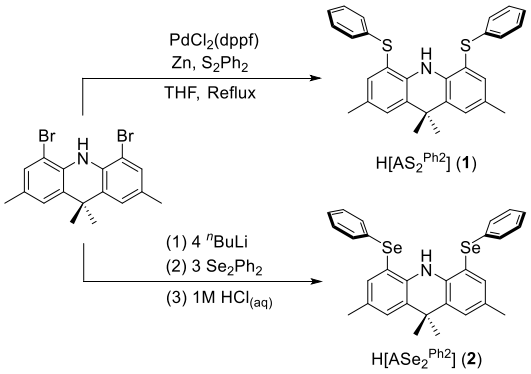

Scheme 1. Syntheses of the H[AS_2^{Ph2}] (**1**) and H[ASe_2^{Ph2}] (**2**) pro-ligands. Dppf = 1,1'-bis(diphenylphosphino)ferrocene.

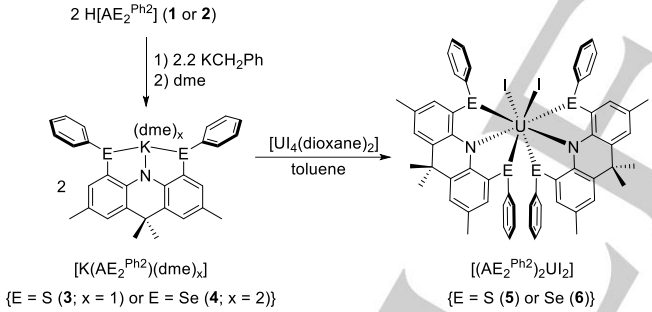

Scheme 2. Syntheses of [K(AE_2^{Ph2})(dme)$_x$] {E = S, x = 1 (**3**) or E = Se, x = 2 (**4**)} and [(AE_2^{Ph2})$_2$$UI_2$] {E = S (**5**) or Se (**6**)}. dme = 1,2-dimethoxyethane; dioxane = 1,4-dioxane.

Reaction of two equivalents of **3** with [UI_4(dioxane)$_2$] in toluene afforded [(AS_2^{Ph2})$_2$$UI_2$] (**5**), which could be isolated in 29% yield as a dark brown powder after filtration in toluene and recrystallization (Scheme 2).[16] Similarly, the reaction of two equivalents of [K(ASe_2^{Ph2})(dme)$_2$] (**4**) with [UI_4(dioxane)$_2$] in toluene, followed by washing with hexanes and recrystallization, afforded dark brown [(ASe_2^{Ph2})$_2$$UI_2$] (**6**) in 52 % yield (Scheme 2). The ^{1}H NMR spectra of **5** and **6** exhibit comparable paramagnetically shifted resonances between –20 ppm and +35 ppm, and are indicative of two equivalent AE_2^{Ph2} ligands lacking side-side and top-bottom symmetry.

X-ray crystal structures of **5**·3.5 toluene (Figure S17) and **6**·1.32 hexane (Figure 2) revealed qualitatively analogous structures with approximate (**5**) or exact (**6**) *C*$_2$ symmetry. The coordination geometry at uranium is distorted square antiprismatic,[17] with each square face occupied by one iodide and one κ^3-coordinated AE_2^{Ph2} ligand.

In the structure of **5**, the acridanide backbones of the AS_2^{Ph2} ligands are bent by 16° and 23°, and the metal is located 1.70 and 1.72 Å below the plane of the SNS donors. The geometry at sulfur is pyramidal, with the sum of the C–S–C and U–S–C angles ranging from 313° to 321° {C–S–C = 102.3(5)-103.6(5)°; U–S–C = 91.5(4)-122.8(4)°}. The U–S distances in **5** range from 2.967(3) to 3.004(3) Å. These distances are within the sum of the covalent radii for sulfur and uranium (3.01 Å),[18] and are shorter than those in most uranium(IV)-thioether complexes {3.089(1) Å in [Cp*U{κ^6-B_3(Cat)$_6$}(SMe$_2$)],[19] 3.04(1) and 3.09(1) Å in [(κ^2-MeSCH$_2$CH$_2$SMe)U(BH_3Me)$_4$],[20] and 3.120(4)-3.275(4) Å in [{($MeBH_3$)$_4$U(μ-THT)}$_2$]}.[21] However, shorter U–S distances {2.763(2), 2.779(2) Å} were previously observed in [(κ^3-TXA_2)UCl_3]$^-$ {TXA_2 = 4,5-bis(2,6-diisopropylanilido)-2,7-di-*tert*-butyl-9,9-dimethylthioxanthene} in which the thioether is incorporated into the backbone of a rigid dianionic NSN-donor ligand.[4]

In the solid-state structure of **6**, the acridanide backbone of the ASe_2^{Ph2} ligands is bent by 30°, and the metal is located 1.76 Å below the plane of the SeNSe donors. The chalcogen donors are more strongly pyramidalized in **6** than in **5**, with the sum of the C–Se–C and U–Se–C angles equal to 299° and 312°. In addition, the C–Se–C bond angles of 97.1(4)-100.4(5)° are slightly more acute than the corresponding angles in **5**, and the U–Se–C angles {89.0(3)° and 93.8(3)°} fall in a much narrower range than the U–S–C angles in **5**, and on average are more acute.

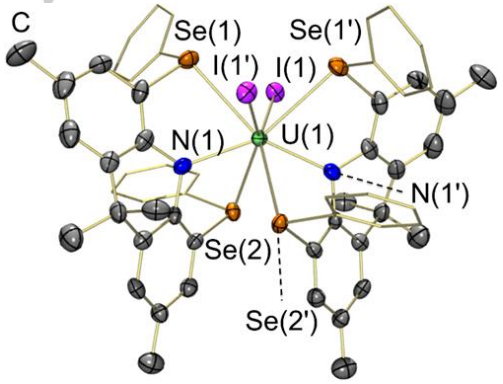

Figure 2. X-ray crystal structure of [(ASe_2^{Ph2})$_2$$UI_2$]·1.32 hexane (**6**·1.32 hexane). Hydrogen atoms and lattice solvent are omitted for clarity, and phenyl rings are shown in wireframe. Ellipsoids are drawn at 50% probability.

The U–Se distances in **6** are 3.049(1) and 3.067(1) Å, which lie well within the sum of the covalent radii for selenium and uranium (3.16 Å).[18] In addition, it is notable that the difference between the shortest U–S bond in **5** and the longest U–Se bond in **6** is 0.10 Å, which is significantly smaller than the difference in the covalent radii of sulfur and selenium (0.15 Å). The U–Se distances in **6** are approximately 0.2 Å longer than the terminal selenolate distances in [U(SePh)$_2$(μ-SePh)$_2$(CH_3CN)$_2$]$_2$ (2.849(1) Å)[22] and [(C_5Me_5)$_2$UMe(SePh)] (2.8432(7) Å).[23] However, they are significantly shorter than the U–Se distances in [{(4,6-^{t}Bu$_2$$C_6H_2$O)$_2$Se}$_2$U(THF)$_2$] (b in Figure 1; 3.1642(6) Å and 3.2606(6) Å),[9] and the U–Se(2) and U–Se(3) distances in the μ-Se_4 ligands in [{({^{Ad}ArO}$_3$N)U(THF)}$_2$(μ-η^2:η^2-Se_4)] (c in Figure 1;

3.178(1) Å) and [{{(^{Ad}ArO)$_3$N}U)$_2$(μ-η^3:η^3-Se$_4$)] (3.121(1) Å and 3.125(1) Å).[12] Additionally, they are only slightly elongated relative to the longer of the two U–Se distances (3.0076(4)-3.0477(7) Å) for each diselenophosphinate ligand in homoleptic uranium(IV) [U(κ^2-Se$_2$PR$_2$)$_4$] (Se$_2$PR$_2$; R = Ph, ^{i}Pr or ^{t}Bu) complexes (d in Figure 1).[13]

The U–N distances in **5** (2.364(9) Å and 2.371(9) Å) and **6** (2.378(9) Å) are equal within error, and fall within the typical range for uranium(IV)–diarylamido complexes.[4,24] The U–I bond distance of 3.068(1) Å in **6** is slightly longer than those in **5** {3.018(1) Å and 3.038(1) Å).

The UV-visible absorption spectra for **5** and **6** (Figure 3; top) are very similar. In the UV region, they exhibit an intense (ε ≈ 30,000 cm^{-1}M^{-1}) broad absorption at 33,110 cm^{-1} (for **5**) or 32,570 cm^{-1} (for **6**). Analogous features are seen in the UV-Visible spectra of H[AS$_2$^{Ph2}] (**1**) and H[ASe$_2$^{Ph2}] (**2**), consistent with a ligand-centred (e.g. π→π* or n→π*) transition. The spectra of the potassium ligand salts, **3**-**4**, are similar to those of **5**-**6**, but with transitions shifted to lower energy; an analogous trend was observed for the potassium salt of the PNP (PNP = bis{2-(diisopropylphosphino)-4-methylphenyl}amido) ligand relative to [(PNP)$_2$UCl$_2$].[24] Each uranium complex also gives rise to several broad medium intensity (ε = 1,000-5,000 cm^{-1}M^{-1}) peaks between 26,000 cm^{-1} and 12,000 cm^{-1}, which are not present in the spectra of **1**-**2** and can be attributed to *f–d* or charge transfer transitions. These peaks in the spectrum of **6** are slightly bathochromically shifted relative to those for **5**. The NIR absoprtion spectra of **5** and **6** are very similar (Figure 3; bottom), displaying at least ten low intensity (ε < 250 cm^{-1}M^{-1}) Laporte forbidden *f–f* transitions which arise from the 5*f*^{2} electronic configuration of uranium(IV); the primary differences in the NIR spectra of **5** and **6** are the relative intensities of the peaks between 10,000 and 8,000 cm^{-1}.

In order to gain insight into the nature of the uranium–chalcogen interactions in **5** and **6**, we turned to DFT calculations (ADF, gas-phase, all-electron, spin-unrestricted, net spin polarization of 2, PBE, D3-BJ, TZ2P, ZORA). The geometry optimized structures of **5** and **6** match well with the X-ray structures, although the geometry is now closer to a triangular dodecahedron than a square antiprism.[17] The U–I, U–N, U–S, and U–Se distances are within 0.04, 0.05, 0.03 and 0.02 Å of the crystallographic values, respectively, and the U–E–C and C–E–C angles are well reproduced (to within 5°).

Calculations on a hypothetical ether analogue of **5** and **6**, [(AO$_2$^{Ph2})$_2$UI$_2$] (**7**), were also carried out with a view towards comparison of U–SR$_2$ and U–SeR$_2$ bonding with U–OR$_2$ bonding. However, these calculations did not converge to a sensible minimum due to unfavourable steric interactions between neighbouring ligands (precipitated by a preference for trigonal planar rather than pyramidal geometry at oxygen). Consequently, DFT calculations were also carried out on analogues of **5**-**7** in which the four methyl groups on each acridanide ligand backbone have been removed: [(AE$_2$^{Ph2*})$_2$UI$_2$] {E = S (**5***), Se (**6***), O (**7***)}.

The AE$_2$^{Ph2*} ligand coordination modes in **5*** and **6*** are analogous to those in **5** and **6**, but the geometry at uranium is now closer to that of a triakis tetrahedron than a square antiprism.[17] Additionally, whereas the U–I distances are essentially unchanged, the U–N distances are shorter by 0.05-0.06 Å, and one of the two U–E distances to each tridentate ligand is elongated by 0.08 Å (in **5***) or 0.05 Å (in **6***); the shorter distance in each case involves the chalcogen approximately *trans* to an amido donor. For **7***, the geometry is intermediate between square antiprismatic and cubic.[17] The U–I distances are 3.074 and 3.075 Å, and the U–N distances are 2.350 and 2.351 Å {which are only slightly shorter than the U–N bonds in **5*** and **6*** (2.360-2.374 Å)}. The geometry around each oxygen donor is trigonal planar, and each ONO-donor ligand has one shorter (2.543 or 2.549 Å; this bond involves the oxygen atom approximately *trans* to an amido donor) and one longer (2.634 or 2.645 Å) U–O distance. These distances fall within the usual range for uranium–ether bonds.[25]

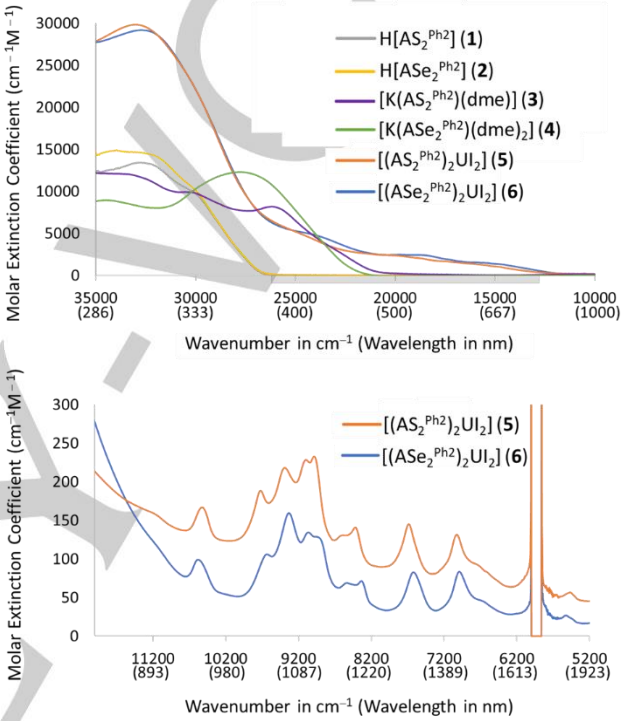

Figure 3. UV-visible spectra (top) of compounds **1**-**6** and NIR spectra (bottom) of **5** (orange) and **6** (blue) in toluene (**1**-**2**, **5**-**6**) or dme (**3**-**4**). The grey bar from ~26,000 to 13,000 cm^{-1} highlights the visible region. The discontinuity in the NIR spectrum between 6,000 and 5,860 cm^{-1} is due to absorbance of the solvent in that region.

Substantial bonding interactions between uranium and the chalcogen donors in **5*** and **6*** are highlighted by average U–S and U–Se Mayer bond orders[26] of 0.38-0.49 and 0.42-0.49, respectively. Additionally, U–O Mayer bond orders of 0.20-0.25 were observed for **7***. For comparison, the U–N and U–I Mayer bond orders in **5***-**7*** range from 0.54-0.58 and 0.81-0.92, respectively. Furthermore, Atoms in Molecules (AIM) bond critical points were located between uranium and each chalcogen donor (*vide infra*).

Increasing covalent character in the U–E bonds along the series **7*** (E = O) < **6*** (E = S) < **5*** (E = Se) is reflected by a number of computational metrics. For example, the Hirshfeld charge[27] on uranium decreases from 0.512 in **7***, to 0.360 in **5*** and 0.326 in **6*** (a in Figure 4). Additionally, the uranium atomic orbital contributions to the Natural Localized Molecular Orbitals (NLMOs; obtained from Natural Bond Order analysis) associated with the U–E bonds (normalized to include U and E contributions only) increase from 3.6-4.9% in **7***, to 9.9-14.4% in **5*** and 11.4-16.6%

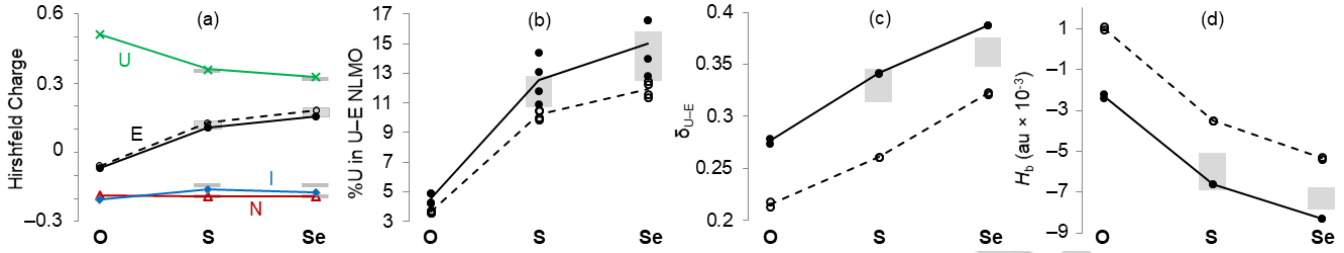

Figure 4. Graphs of computational metrics discussed in the context of U–E bond covalency in $[(AE_2^{Ph2*})_2UI_2]$ {E = O (**7***), S (**5***), Se (**6***)}. (a) Hirshfeld charges on U, E, N and I. (b) % Uranium character in the NLMOs associated with the U–E bonds (normalized to include U and E contributions only). (c) AIM bond-delocalization index for U–E interactions (δ_{U-E}). (d) Total energy of Cremer and Kraka at the U–E bond critical point (H_b). Circles, crosses, triangles, or diamonds represent data for **5***-**7***. Each ENE-donor ligand in the structures of **5***-**7*** features one shorter and one longer U–E bond; filled circles correspond to the shorter of these bonds (or, for graph a, E in these bonds), whereas empty circles correspond to the longer of these bonds (or, for graph a, E in these bonds); solid black lines represent an average of values depicted by filled circles, and dashed black lines correspond to an average of values depicted by empty circles. For comparison, grey rectangles indicate the range of values for $[(AE_2^{Ph2})_2UI_2]$ {E = S (**5**) and Se (**6**)}.

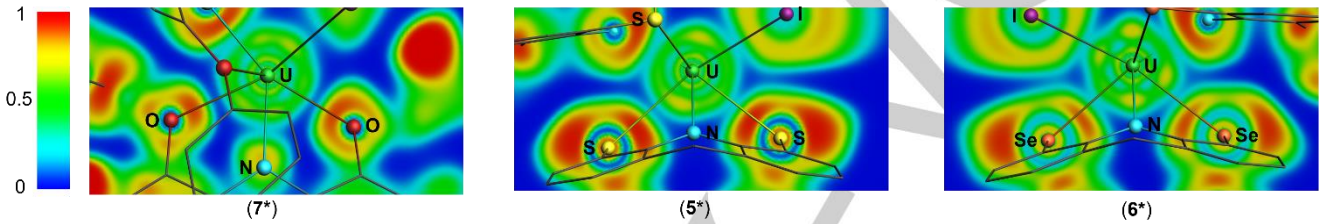

Figure 5. Slice of the Electron Localization Function (ELF) in the E–U–E plane associated with one ENE-donor ligand in **5***-**7*** (ELF values are an average of those generated from alpha and beta spin). Atoms not shown in wireframe are coloured as follows: U = green, N = blue, I = purple, O = red, S = yellow, and Se = orange.

in **6*** (b in Figure 4).[28] This uranium contribution is dominated by 6*d* (33.7-50.4%) and 5*f* (33.1-53.4%) character.

Atoms in Molecules (AIM) calculations[29] have commonly been used to analyze the nature of bonding interactions, including those involving uranium.[4,30,31] In particular, the bond delocalization index ($\delta_{(A-B)}$)[32] and the total energy density of Cremer and Kraka at the bond critical point (H_b)[33] are useful for the analysis of bonds involving atoms with diffuse valence electrons, as well as weak or strongly polar bonds. In **5***-**7***, the U–E bond delocalization index (c in Figure 4) increases in the order **7*** (E = O) < **6*** (E = S) < **5*** (E = Se), indicative of increasing electron sharing. Additionally, H_b at the U–E bond critical points (d in Figure 4) decreases in the order **7*** > **6*** > **5***, with negative values observed for all U–S and U–Se bonds, indicative of appreciable covalency.

Analogous trends were observed for unmodified **5** and **6**,[34] and the range of Hirshfeld charge, %U character in U–E NLMO, δ_{U-E}, and H_b values for **5** and **6** are illustrated by the grey rectangles in the background of Figure 4.

Electron Localization Function (ELF) calculations were also carried out (ELF calculations provide a means to map electron pair probability; higher ELF values along the trajectory between two atoms are generally indicative of a more covalent bond).[35] Figure 5 shows ELF values in the E–U–E plane associated with one of the two AE_2^{Ph2*} ligands in **5***-**7***. These plots reveal prominent regions of low ELF values (shown in dark blue) for the U–O bonds in **7***, whereas such regions are less pronounced or absent for the U–S and U–Se bonds in **5*** and **6***. These data are consistent with increased covalency[31,36] in the U–SR_2 and U–SeR_2 bonds relative to the U–OR_2 bonds.

In summary, a novel rigid SeNSe-donor pincer ligand has been used to access the first example of a uranium–selenoether complex, $[(ASe_2^{Ph2})_2UI_2]$, highlighting the feasibility of accessing uranium–selenoether interactions through ligand design. The thioether analogue was also prepared, and DFT calculations on the selenoether and thioether complexes, as well as methyl-free structures and a hypothetical ether analogue, indicate increasing U–E covalency from O to S to Se. These findings suggest the potential utility of selenoether-containing ligand systems in lanthanide-actinide separation.

Crystallographic Details

Deposition Numbers 2112402 (for **5**·3.5 toluene) and 2112404 (for **6**·1.32 hexane) contain the supplementary crystallographic data for this paper. These data are provided free of charge by the joint Cambridge Crystallographic Data Centre and Fachinformationszentrum Karlsruhe Access Structures service.

Acknowledgements

D. J. H. E. thanks NSERC of Canada for a Discovery Grant, and Compute Canada for a 2020 Resources for Research Groups (RRG) grant. Also, we are grateful to Dr. Daniel B. Leznoff and Dr. Wen Zhou at Simon Fraser University for assistance with elemental analysis, Dr. Ignacio Vargas-Baca and Dr. Paul W. Ayers at McMaster University for advice with DFT calculations, and Dr. James F. Britten in the McMaster X-ray diffraction facility for helpful crystallographic discussions.

Keywords: uranium • selenoether • thioether • bonding • covalency

[1] A. Leoncini, J. Huskens, W. Verboom, *Chem. Soc. Rev.* **2017**, *46*, 7229-7273.

[2] a) N. P. Bessen, J. A. Jackson, M. P. Jensen, J. C. Shafer, *Coord. Chem. Rev.* **2020**, *421*, 213446; b) I. Lehman-Andino, J. Su, K. E. Papathanasiou, T. M. Eaton, J. W. Jian, D. Dan, T. E. Albrecht-Schmitt, C. J. Dares, E. R. Batista, P. Yang, J. K. Gibson, K. Kavallieratos, *Chem. Commun.* **2019**, *55*, 2441-2444; c) N. Bessen, Q. Yan, N. Pu, J. Chen, C. Xu, J. Shafer, *Inorg. Chem. Front.* **2021**, *8*, 4177-4185.

[3] M. Ephritikhine, *Coord. Chem. Rev.* **2016**, *319*, 35-62.

[4] B. Vidjayacoumar, S. Ilango, M. J. Ray, T. Chu, K. B. Kolpin, N. R. Andreychuk, C. A. Cruz, D. J. H. Emslie, H. A. Jenkins, J. F. Britten, *Dalton Trans.* **2012**, *41*, 8175-8189.

[5] a) S. X. Hu, J. J. Liu, J. K. Gibson, J. Li, *Inorg. Chem.* **2018**, *57*, 2899-2907; b) N. P. Bessen, I. A. Popov, C. R. Heathman, T. S. Grimes, P. R. Zalupski, L. M. Moreau, K. F. Smith, C. H. Booth, R. J. Abergel, E. R. Batista, P. Yang, J. C. Shafer, *Inorg. Chem.* **2021**, *60*, 6125-6134; c) B. Sadhu, M. Dolg, *Inorg. Chem.* **2019**, *58*, 9738-9748; d) C. Wang, Q. Y. Wu, X. H. Kong, C. Z. Wang, J. H. Lan, C. M. Nie, Z. F. Chai, W. Q. Shi, *Inorg. Chem.* **2019**, *58*, 10047-10056; e) E. M. Matson, A. T. Breshears, J. J. Kiernicki, B. S. Newell, P. E. Fanwick, M. P. Shores, J. R. Walensky, S. C. Bart, *Inorg. Chem.* **2014**, *53*, 12977-12985; f) M. P. Jensen, A. H. Bond, *J. Am. Chem. Soc.* **2002**, *124*, 9870-9877; g) M. W. Rosenzweig, J. Hummer, A. Scheurer, C. A. Lamsfus, F. W. Heinemann, L. Maron, M. Mazzanti, K. Meyer, *Dalton Trans.* **2019**, *48*, 10853-10864; h) R. D. M. Greer, C. Celis-Barros, J. M. Sperling, A. N. Gaiser, C. J. Windorff, T. E. Albrecht-Schonzart, *Inorg. Chem.* **2020**, *59*, 16291-16300; i) C. A. P. Goodwin, A. W. Schlimgen, T. E. Albrecht-Schönzart, E. R. Batista, A. J. Gaunt, M. T. Janicke, S. A. Kozimor, B. L. Scott, L. M. Stevens, F. D. White, P. Yang, *Angew. Chem. Int. Ed.* **2021**, *60*, 9459-9466; j) M. L. Tarlton, O. J. Fajen, S. P. Kelley, A. Kerridge, T. Malcomson, T. L. Morrison, M. P. Shores, X. Xhani, J. R. Walensky, *Inorg. Chem.* **2021**, *60*, 10614-10630.

[6] A. J. Gaunt, S. D. Reilly, A. E. Enriquez, B. L. Scott, J. A. Ibers, P. Sekar, K. I. M. Ingram, N. Kaltsoyannis, M. P. Neu, *Inorg. Chem.* **2008**, *47*, 29-41.

[7] a) M. L. Neidig, D. L. Clark, R. L. Martin, *Coord. Chem. Rev.* **2013**, *257*, 394-406; b) K. A. Pace, V. V. Klepov, A. A. Berseneva, H. C. zur Loye, *Chem. Eur. J.* **2021**, *27*, 5835-5841.

[8] A. J. Gaunt, B. L. Scott, M. P. Neu, *Chem. Commun.* **2005**, 3215-3217.

[9] A. J. Myers, P. Rungthanaphatsophon, A. C. Behrle, S. P. Vilanova, S. P. Kelley, W. W. Lukens, J. R. Walensky, *Chem. Commun.* **2018**, *54*, 10435-10438.

[10] The thorium complex, [{(4,6-^{t}Bu$_2$C$_6$H$_2$O)$_2$Se}$_2$Th(THF)$_2$], was reported prior to the uranium analogue, and the authors suggested a Th–Se interaction on the basis of the ^{77}Se NMR chemical shift: A. C. Behrle, J. R. Levin, J. E. Kim, J. M. Drewett, C. L. Barnes, E. J. Schelter, J. R. Walensky, *Dalton Trans.* **2015**, *44*, 2693-2702.

[11] L. P. Spencer, P. Yang, B. L. Scott, E. R. Batista, J. M. Boncella, *Inorg. Chem.* **2009**, *48*, 11615-11623.

[12] S. M. Franke, F. W. Heinemann, K. Meyer, *Chem. Sci.* **2014**, *5*, 942-950.

[13] a) M. B. Jones, A. J. Gaunt, J. C. Gordon, N. Kaltsoyannis, M. P. Neu, B. L. Scott, *Chem. Sci.* **2013**, *4*, 1189-1203; b) A. C. Behrle, A. Kerridge, J. R. Walensky, *Inorg. Chem.* **2015**, *54*, 11625-11636.

[14] Uranium(IV) diselenophosphonate {Se$_2$PR(OR)} complexes have been synthesized, but were not crystallographically characterized. A thioselenophosphinate complex, [U(SSePPh$_2$)$_4$] was also reported, but the solid state structure suffered from S/Se disorder: A. C. Behrle, C. L. Barnes, N. Kaltsoyannis, J. R. Walensky, *Inorg. Chem.* **2013**, *52*, 10623-10631.

[15] S.-i. Fukuzawa, D. Tanihara, S. Kikuchi, *Synlett* **2006**, *13*, 2145-2147.

[16] Compound **5** was also formed via the reaction of one equivalent of Li[AS$_2^{Ph2}$] with UI$_3$ in benzene or dme, presumably via disproportionation.

[17] Geometries were assigned through the use of continuous shape measure (CSM) analysis using the SHAPE program: H. Zabrodsky, S. Peleg, D. Avnir, *J. Am. Chem. Soc.* **1992**, *114*, 7843-7851. Details are provided in the supporting information.

[18] B. Cordero, V. Gómez, A. E. Platero-Prats, M. Revés, J. Echeverría, E. Cremades, F. Barragán, S. Alvarez, *Dalton Trans.* **2008**, 2832-2838.

[19] E. Barnea, T. Andrea, M. Kapon, M. S. Eisen, *J. Am. Chem. Soc.* **2004**, *126*, 5066-5067.

[20] R. Shinomoto, A. Zalkin, N. M. Edelstein, D. Zhang, *Inorg. Chem.* **1987**, *26*, 2868-2872.

[21] R. Shinomoto, A. Zalkin, N. M. Edelstein, *Inorg. Chim. Acta* **1987**, *139*, 91-95.

[22] A. J. Gaunt, B. L. Scott, M. P. Neu, *Inorg. Chem.* **2006**, *45*, 7401-7407.

[23] W. J. Evans, K. A. Miller, J. W. Ziller, A. G. DiPasquale, K. J. Heroux, A. L. Rheingold, *Organometallics* **2007**, *26*, 4287-4293.

[24] T. Cantat, B. L. Scott, D. E. Morris, J. L. Kiplinger, *Inorg. Chem.* **2009**, *48*, 2114-2127.

[25] 97.5% of the U–OR$_2$ distances in the CSD fall within the range 2.31-2.76 Å. CSD accessed via Conquest (CSD version 5.42, updated November 2020).

[26] A. J. Bridgeman, G. Cavigliasso, L. R. Ireland, J. Rothery, *J. Chem. Soc., Dalton Trans.* **2001**, 2095-2108.

[27] C. F. Guerra, J. W. Handgraaf, E. J. Baerends, F. M. Bickelhaupt, *J. Comput. Chem.* **2004**, *25*, 189-210.

[28] NBO calculations on **5***, **6***, and **7*** each yielded eight NLMOs associated with U–E bonds (four chalcogen donors per complex, each with an alpha- and a beta-spin orbital). Assignment of NLMOs as bonding NLMOs was based on intuitive analysis of the orbital isosurface and percentage uranium character, rather than the program-generated descriptor.

[29] R. F. Bader, *Atoms in Molecules: A Quantum Theory*, Clarendon, New York, **1990**.

[30] a) M. J. Tassell, N. Kaltsoyannis, *Dalton Trans.* **2010**, *39*, 6719-6725; b) D. M. King, F. Tuna, E. J. L. McInnes, J. McMaster, W. Lewis, A. J. Blake, S. T. Liddle, *Nat. Chem.* **2013**, *5*, 482-488; c) B. M. Gardner, G. Balazs, M. Scheer, F. Tuna, E. J. L. McInnes, J. McMaster, W. Lewis, A. J. Blake, S. T. Liddle, *Angew. Chem. Int. Ed.* **2014**, *53*, 4484-4488; d) Q. R. Huang, J. R. Kingham, N. Kaltsoyannis, *Dalton Trans.* **2015**, *44*, 2554-2566; e) J. P. Dognon, *Coord. Chem. Rev.* **2017**, *344*, 150-162; f) M. Zegke, X. B. Zhang, I. Pidchenko, J. A. Hlina, R. M. Lord, J. Purkis, G. S. Nichol, N. Magnani, G. Schreckenbach, T. Vitova, J. B. Love, P. L. Arnold, *Chem. Sci.* **2019**, *10*, 9740-9751.

[31] Q. Y. Wu, J. H. Lan, C. Z. Wang, Y. L. Zhao, Z. F. Chai, W. Q. Shi, *J. Phys. Chem. A* **2015**, *119*, 922-930.

[32] C. F. Matta, R. J. Boyd, in *The Quantum Theory of Atoms in Molecules* (Eds: C. F. Matta, R. J. Boyd), Wiley-VCH, Weinheim, **2007**, pp. 1-33.

[33] a) D. Cremer, E. Kraka, *Croat. Chem. Acta* **1984**, *57*, 1259-1281; b) D. Cremer, E. Kraka, *Angew. Chem. Int. Ed. Engl.* **1984**, *23*, 627-628.

[34] The U–E bond distances (and Mayer bond orders) are 2.97-3.01 Å (0.45-0.50) in **5** and 3.06-3.07 Å (0.47-0.49) in **6**. Hirshfeld charges on uranium are 0.353 in **5** and 0.320 in **6**. Uranium atomic orbital contributions to the NLMOs associated with the U–E bonds are 10.7-12.8% in **5** (36.7-51.7% 6*d*, 31.4-43.7% 5*f*) and 12.5-15.8% in **6** (39.3-53.6% 6*d*, 26.2-49.9% 5*f*). AIM U–E bond delocalization indices are 0.312-0.346 in **5** and 0.348-0.376 in **6**. The total energy density of Cremer and Kraka at the U–E bond critical point (H_b) ranges from –0.0051 to –0.0069 au in **5** and –0.0066 to –0.0077 au in **6**.

[35] a) P. Fuentealba, E. Chamorro, J. C. Santos, in *Theoretical and Computational Chemistry,* Vol. 19 (Ed: A. Toro-Labbé), Elsevier, **2007**, pp. 57-85; b) Y. Grin, A. Savin, B. Silvi, in *The Chemical Bond: Fundamental Aspects of Chemical Bonding* (Eds: G. Frenking, S. Shaik), Wiley-VCH Verlag, **2014**, pp. 345-382; c) K. Koumpouras, J. A. Larsson, *J. Phys.: Condens. Matter* **2020**, *32*, 315502.

[36] S. F. Matar, *Z. Naturforsch. B* **2017**, *72*, 725-730.

Entry for the Table of Contents

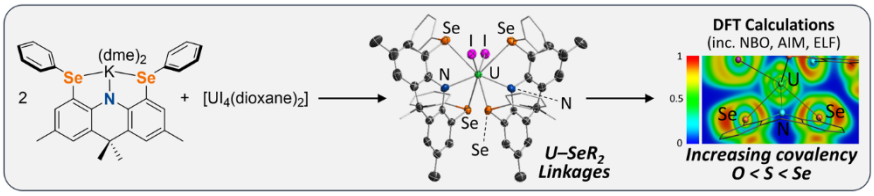

Table of Contents Text:

Actinide–soft donor linkages are of importance in the context of lanthanide-actinide separation. The first example of a uranium selenoether complex has been prepared through the use of a rigid SeNSe-donor pincer ligand. The thioether analogue was also synthesized. Computational studies, including NBO, AIM and ELF calculations, revealed increasing covalency in U–ER_2 bonding from O to S to Se.